Interference phenomenon and geometric phase for Dirac neutrino in π^+ decay*

J. Syska, J. Dajka, and J. Łuczka
Institute of Physics, University of Silesia, 40-007 Katowice, Poland

We analyze the geometric phase in the neutrino oscillation phenomenon, which follows the pion decay $\pi^+ \to \mu^+ + \nu_\mu$. Its value π is consistent with the present-day global analysis of the Standard Model neutrino oscillation parameters, accounting for the nonzero value of θ_{13}. The impact of the charge-parity (CP) violating phase δ, the neutrino's nature, and the new physics is discussed.

PACS numbers: 14.60 Pq, 03.65.Vf

arXiv:1309.7536v1 [hep-ph] 29 Sep 2013

I. Introduction. The aim of this brief paper is to discuss the idea that in measurement subtleties of the neutrino oscillation phenomenon, geometrical properties reflected in the geometric phase of the oscillating flavor neutrino are important. In Ref. [1] it was proposed that the production and detection of the neutrino shall be treated as the split-beam experiment in the energy space. In the present paper, we consider the muon neutrino which is produced in the decay of pion to muon and the Dirac neutrino, namely $\pi^+ \to \mu^+ + \nu_\mu$ [2]. The flavor neutrino state $|\nu_\mu\rangle$ is a superposition of the stationary states $|\nu_i\rangle_\lambda \equiv |p, \lambda, i\rangle$ of the definite masses m_i, $i = 1, 2, 3$, helicities $\lambda = -1$ or $+1$, and four-momentum p. When the new physics (NP) interactions are included, this superposition composes the mixed state [3, 4]. Thus, the flavor neutrino, here ν_μ, represents the beam of three massive states, which split at the moment of production of the $\alpha = \mu$-flavor superposition, propagate, and finally at the distance L, interfere in the detector in the β-flavor interference pattern. This interference experiment for the neutrino proposed in [1] and discussed in [1, 5] in two flavor neutrino cases, allows us to test the dependence of the type [6] of the Aharonov-Anandan geometric phase (GP) [7] on the particular field theory model to which this paper is devoted.

The global analysis of neutrino oscillation parameters [8] shows the discrepancy in the data for the atmospheric neutrino mixing angle θ_{23}. For the normal neutrino mass ordering (and we will use this one), the profile of the $\Delta\chi^2$ test statistics has two almost equally deep minima–the "local minimum" (lm) for the solar plus reactor long-baseline and accelerator long-baseline neutrino experiments, with new data from the ν_μ and $\bar{\nu}_\mu$ channels included, and the "global minimum" (gm), which includes data from atmospheric neutrinos, too. The profile is practically symmetric and the preference (if any, see [9]) of gm (with $\sin^2\theta_{23} = 0.427$) over lm (with $\sin^2\theta_{23} = 0.613$) is very weak as the difference of $\Delta\chi^2$ in these minima is equal to 0.02 [8]. The 2σ range $(0.38, 0.66)$ covers both of them. The experimental reason is that θ_{23} strongly depends on the CP violating phase δ [9], whose 1σ range is $\langle 0, 2\pi)$ [8]. For further discussion of this problem, see [10, 11]. It will appear that the mean $\sin^2\theta_{23} \approx 0.517$ is the robust one. The central values of the other oscillation parameters are [8] $\sin^2\theta_{12} = 0.320$, $\sin^2\theta_{13} = 0.0246$, $\delta = 0.80\,\pi$, $\Delta m^2_{21} = 7.62 \times 10^{-5} eV^2$ and $\Delta m^2_{31} = 2.55 \times 10^{-3} eV^2$.

A. Muon neutrino density matrix: From the $\pi^+ \to \mu^+ + \nu_\mu$ decay experiments [2], we know that the fraction of the right-handed $N_{\nu_{+1}}$ to the left-handed $N_{\nu_{-1}}$ neutrinos fulfils the constraint [12, 13]

$$N_{\nu_{+1}}/N_{\nu_{-1}} < 0.002\,. \tag{1}$$

Let us assume that the pion decays effectively both in the left (L) and right (R) chiral charge current (CC) interactions [4] via the exchange of the Standard Model (νSM) W boson only. Then, at the W-boson energy scale, the R and L chiral pion decay constants [14] are equal [15]. Moreover, the pseudoscalar correction to the pion hadronic matrix element can be neglected due to its smallness [16]. Then the invariant amplitudes $A_i^{\mu\ \lambda;\lambda_\mu}(p)$ in the decay $\pi^+ \to \mu^+ + \nu_{i,\lambda}$ are related as follows [2, 4],

$$|A_i^{\mu\ +1;+1}(p)|^2 = |A_i^{\mu\ -1;-1}(p)|^2\, \frac{|\varepsilon_R|^2 |U^R_{\mu i}|^2}{|\varepsilon_L|^2 |U^L_{\mu i}|^2}\,. \tag{2}$$

Here, $U^L_{\alpha i}$ and $U^R_{\alpha i}$ are the L and R chiral neutrino mixing matrices, which enter into the CC Lagrangian in the products with the coupling constants ε_L and ε_R, respectively [4]. The NP values of ε_L and ε_R can deviate slightly from the νSM values 1 and 0, respectively. However, the Fermi constant constraint $\varepsilon_L^4 + \varepsilon_R^4 = 1$ should hold.

Under the above conditions, in the process of neutrino production (P) the nonzero neutrino density matrix elements in the mass-helicity basis $|\nu_i\rangle_\lambda$ and in the center-of-mass (CM) frame are as follows [3, 4]:

$$\varrho^{\mathrm{P}\mu\ i;\,i'}_{-1;\,-1} = \frac{|\varepsilon_L|^2 U^{L*}_{\mu i} U^L_{\mu i'}}{|\varepsilon_R|^2 + |\varepsilon_L|^2},\ \varrho^{\mathrm{P}\mu\ i;\,i'}_{+1;\,+1} = \frac{|\varepsilon_R|^2 U^{R*}_{\mu i} U^R_{\mu i'}}{|\varepsilon_R|^2 + |\varepsilon_L|^2}\,, \tag{3}$$

constituting the muon neutrino 6×6-dimensional block diagonal density matrix $\rho^{\mathrm{P}\mu} = \mathrm{diag}(\varrho^{\mathrm{P}\mu}_{-1;\,-1}, \varrho^{\mathrm{P}\mu}_{+1;\,+1})$ with two 3×3 matrices given in (3). Here we choose $U^R_{\alpha i} = U^L_{\alpha i} = U_{\alpha i}$, where U is the Maki-Nakagawa-Sakata neutrino mixing matrix [17], as the full statistical analysis of this hypothesis is beyond the data accessible

* Published in: Phys.Rev.D **87**, 117302 (2013);
DOI: 10.1103/PhysRevD.87.117302

in the present-day experiments. Using (1) we obtain the bound on the ratio $|\varepsilon_R/\varepsilon_L| < 0.0447$. It constrains the density matrix $\varrho^{\mathrm{P}\mu\, i;\, i'}_{+1;+1}$ of the initial neutrino. Its evolution and the effective Hamiltonian during the neutrino propagation are described in the next section. Next, for the neutrino energy $E_\nu > 100$ MeV, the neutrino is in practice the relativistic particle. Hence the effect of the helicity Wigner rotation is negligible [3] and the result for the density matrix in the laboratory (**L**) frame is $\varrho^{\mathrm{P}}_{\mathbf{L}}(\vec{p}_{\mathbf{L}}) = \varrho^{\mathrm{P}}(\vec{p})$. Finally, only the neutrino which is produced in the **L** frame in the forward direction along the z axis reaches the detector and we choose this axis as the quantization one.

II. Evolution of the density matrix. Under the requirement of the nondissipative homogeneous medium, the Liouville-von Neumann equation governs the density matrix evolution. Thus, in the ultrarelativistic case, when the distance and the propagation time approach the relation $z = t$, the evolution rule for the neutrino density matrix is as follows:

$$\rho^{\mu}(t=0) \to \rho^{\mu}(t) = e^{-i\,\mathcal{H}\,t}\rho^{\mathrm{P}\mu}(t=0)\; e^{i\,\mathcal{H}\,t}\,, \qquad (4)$$

where $\rho^{\mathrm{P}\mu}$ is an initial density matrix (3) and $\mathcal{H}$ is the effective Hamiltonian.

With three massive and two helicity neutrino states, the effective Hamiltonian $\mathcal{H}$ has the 6×6-dimensional representation. In the case of the axial-vector interactions only, the effective Hamiltonian $\mathcal{H}$ can be considered as block diagonal with two 3×3 matrices,

$$\mathcal{H} = \mathcal{M} + \mathrm{diag}(\mathcal{H}_{--}, \mathcal{H}_{++})\,. \qquad (5)$$

Here $\mathcal{M} = \mathrm{diag}(E^0_1, E^0_2, E^0_3, E^0_1, E^0_2, E^0_3)$ with $E^0_i = E_\nu + m^2_i/2E_\nu$ $(i = 1, 2, 3)$ is the mass term, where E_ν is the energy for the massless neutrino [2]. The interaction Hamiltonians for the coherent Dirac neutrino scattering inside unpolarized matter read [2, 4, 18]

$$\begin{aligned}(\mathcal{H}_{--})_{ij} &= \sqrt{2}G_F N_e|\varepsilon_L|^2\; U^{L*}_{ei}\; U^{L}_{ej} \qquad (6)\\ (\mathcal{H}_{++})_{ij} &= \sqrt{2}G_F\left\{N_e|\varepsilon_R|^2\; U^{R*}_{ei}\; U^{R}_{ej} - \frac{\rho}{2}N_n\,\varepsilon^{N\nu}_R\Omega^R_{ij}\right\},\end{aligned}$$

where N_e and N_n stand for the number of background electrons (e) and neutrons (n) per unit volume, respectively and $\varrho \simeq 1$. Small NP deviations of the neutral coupling constant for background particles are also neglected. We choose the right chiral neutral mixing matrix in the mass basis equal to $\Omega^R = 3\,\mathrm{diag}(w_1, w_2, w_3)$ with $w_{1,2,3} = m_{e,\mu,\tau}/(m_e + m_\mu + m_\tau)$, where m_α, $\alpha = e, \mu, \tau$, is the mass of electron, muon and tau lepton, respectively. The bound on the neutrino right chiral neutral current (NC) coupling constant equal to $|\varepsilon^{N\nu}_R| = 1$ can be obtained from the analysis of the charge-parity-time reversal (CPT) symmetry violation in the neutrino oscillation survival events [19]. In the analysis we assume that the relevant νSM and NP coupling constants are real.

III. Analysis of geometric phase. Various types of geometric phases have been studied for a long time in physical systems ranging from classical mechanics to high-energy physics [20]. There are also examples of exploiting the notion of geometric phases in neutrino physics. Let us mention a few of them. In [21], it was shown that in the neutrino oscillations analysis, carried out under adiabatic conditions [2], the nonzero Berry phase [22] appears in the νSM if a background consists of at least two varying densities. The case of the three-level neutrino systems was considered in [23]. In [1] it was noted that the Pancharatnam phase [24], which defines the relative phases between states in the Hilbert space, leads in two-flavor neutrino oscillation to the topological phase of the interference term, which is equal to zero or π for the survival and appearance probability, respectively.

In the present case, the neutrino ν_μ is produced in the π^+ decay and propagates in the ordinary matter of the crust (with the density $\rho = 2.6$ g/cm^3). It reaches the detector after one oscillation period, i.e. at the maximum of the survival transition rate $P(\nu_\mu \to \nu_\mu)$. If the detector lies at the distance $L = 800$ km which is the baseline for the NOνA–Low-Z Calorimeter experiment [2], it happens for $E_\nu = 0.803$ GeV (what matters is the ratio L/E_ν). For the central value of the CP violating phase $\delta = 0.80\,\pi$ of the U-matrix, we obtain $P(\nu_\mu \to \nu_\mu) \approx 0.992$ (gm) or $P(\nu_\mu \to \nu_\mu) \approx 0.991$ (lm). For perfect cyclicity $P(\nu_\mu \to \nu_\mu) = 1$. Hence the evolution is not exactly cyclic. Another measure of the deviation from perfect cyclicity is the trace distance between initial state at $t = 0$ and the state at time $t = L$ [25],

$$D = \frac{1}{2}||\rho^{\mu}(t=0) - \rho^{\mu}(t=L)||\,, \qquad (7)$$

where the norm $||\varrho|| = \mathrm{Tr}\sqrt{\varrho^\dagger\varrho}$. For perfectly cyclic evolution, $D = 0$. The calculations show that depending on δ and at the central values of other parameters [8], the trace distance $D \in (0.012, 0.092)$ (gm) with the minimum for $\delta = 0$ and maximum for $\delta = \pi$ (the cases when CP is not violated). For $\delta = 0.80$ the minimal value $D = 0.089$ (gm) is at $L = 800$ km, which is the period of the oscillation. The same is true for the "local minimum" [8, 9]. The deviation from the perfect cyclicity is due to the fact that the neutrino flavor state is a three-state system and is not an eigenvector of the effective Hamiltonian governing its propagation.

In this paper, we exploit the kinematic approach to the geometric phase [6] which can be applied to arbitary (also nonunitary and/or noncyclic) quantum evolution. It possesses the following fundamental features [6]: it is gauge invariant, purification independent, and it reduces to well establish results in the limit of unitary evolution. This approach has already been utilized in [5] for the two-flavor neutrino system both for nondissipative and dissipative cases.

In order to analyze the GP, it is convenient to present the density matrix (4) in the spectral-decomposition form

$$\rho^{\mu}(t) = \sum_{i=1}^{6} \lambda_i^{\mu}(t)\, |w_i^{\mu}(t)\rangle\langle w_i^{\mu}(t)|, \qquad (8)$$

where $\lambda_i^{\mu}(t)$ and $|w_i^{\mu}(t)\rangle$ are the eigenvalues and eigenvectors of the matrix $\rho^{\mu}(t)$. Then the geometric phase $\Phi^{\mu}(t)$ at time t associated with such an evolution is defined by the following relation [6]:

$$\Phi^{\mu}(t) \;=\; \mathrm{Arg}\left[\sum_{d=1}^{6} [\lambda_d^{\mu}(0)\lambda_d^{\mu}(t)]^{1/2}\langle w_d^{\mu}(0)|w_d^{\mu}(t)\rangle \times \exp(-\int_0^t \langle w_d^{\mu}(s)|\dot{w}_d^{\mu}(s)\rangle ds)\right], \qquad (9)$$

where $\mathrm{Arg}\,[Z]$ denotes argument of the complex number Z, $\langle w_d^{\mu}|w_d^{\mu}\rangle$ is a scalar product, and the dot indicates the derivative with respect to time s. It is natural to analyze the GP at time $t = L$, which corresponds to the period of neutrino oscillations. Below, we study the GP at this time and use the notation $\Phi \equiv \Phi^{\mu}(t = L)$.

In [1] it was assumed that neutrino oscillation realizes a kind of interference experiment, and under this assumption it was proven that in the two-flavor case, the topological phase of the interference term is reflected in the orthogonality of the mixing matrix. In the present paper, it is suggested that because this interference experiment reflects the orthogonality of the neutrino mixing matrix, the GP takes the topological value π (the correction from the CP violating phase δ will appear very tiny). This value of GP influences self-consistently the parameters of the mixing matrix.

A. Geometric phase in νSM: Because of the mentioned discrepancy in the data, the analysis of the GP given by Eq.(9) is for νSM performed for lm and gm [8]. The results are presented in Fig. 1. The GP for the central values of lm and gm are equal to $\Phi^{lm} = 1.1917\,\pi$ and $\Phi^{gm} = 0.8301\,\pi$, respectively. The bottom line is plotted for $\sin^2\theta_{23} = 0.461$ for $+1\sigma$ bound of lm range $(0.400, 0.461)$ and the upper one for $\sin^2\theta_{23} = 0.573$ for -1σ bound of gm range $(0.573, 0.635)$ [8]. We notice that (with other oscillation parameters fixed) Φ changes linearly as the function of $\sin^2\theta_{13}$, where θ_{13} is the third mixing angle of U [2]. Two examples of the GP solution with $\Phi = \pi$ are pointed out, the first one for $\sin^2\theta_{23} = 0.517$ ($s1$) and the second one for $\sin^2\theta_{23} = 0.514$ ($s2$). The former value, $\sin^2\theta_{23} = 0.517$, is the arithmetic mean of the $+1\sigma$ bound 0.461 for lm and -1σ bound 0.573 for gm. With this value, the condition of the geometric value $\Phi = \pi$ for the GP gives $\sin^2\theta_{13} \approx 0.029$, which lies in the 2σ range (0.019, 0.030) for $\sin^2\theta_{13}$ [8]. In the second example the current central value $\sin^2\theta_{13} = 0.0246$ is chosen. Now, the "GP solution" for $\Phi = \pi$ is $\sin^2\theta_{23} = 0.514$ ($s2$) [11]. The value π of the GP arises as the result of the interference

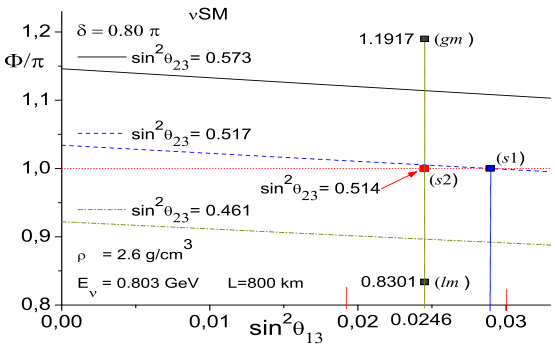


FIG. 1: The geometric phase $\Phi \equiv \Phi^{\mu}(t = L)$ vs $\sin^2\theta_{13}$ plotted for the value of $\sin^2\theta_{23} = 0.461$ ($+1\sigma$ bound lm) and $\sin^2\theta_{23} = 0.573$ (-1σ bound gm) [8]. For any $\sin^2\theta_{13}$ the whole area on the figure is covered by the 2σ range for $\sin^2\theta_{23}$. The GP, 1.1917, and 0.8301, for the central values of gm and lm, respectively, are signified. Two examples of the GP solution are pointed out, $\sin^2\theta_{23} = 0.517$ ($s1$) and $\sin^2\theta_{23} = 0.514$ ($s2$). The $\pm 2\sigma$ limits, 0.019 and 0.030, for $\sin^2\theta_{13}$ are signified by the short vertical lines.

of the neutrino mass states [1] at the point of the flavor neutrino detection at the first period.

The GP changes mainly with $\sin^2\theta_{23}$ and $\sin^2\theta_{13}$ (see Fig. 1), whereas the impact of the other νSM oscillation parameters is significantly weaker. That is, the change of $\Delta^2 m_{31} \equiv m_3^2 - m_1^2$, $\Delta^2 m_{21} \equiv m_2^2 - m_1^2$ and $\sin^2\theta_{12}$ in their 2σ ranges [8] causes the change of Φ/π approximately equal to 3×10^{-4}, 10^{-5}, and 3×10^{-6}, respectively. The small dependence on the CP-violating phase δ is presented in Fig. 2. Its impact is of the order of 10^{-4}. The numerical calculations show that in νSM with the period $L = 800$ km the GP takes the topological values $\Phi^{\mu} = n\ \pi\ (\mathrm{mod}\, 2\,\pi)$, $n \in N$ (up to the influence of the phase δ).

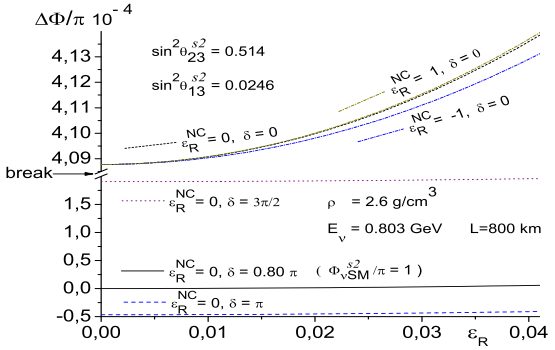


FIG. 2: The geometric phase difference $\Delta\Phi = \Phi_{NP} - \Phi_{\nu\mathrm{SM}}$ as a function of the NP coupling constant ε_R. Each curve corresponds to one δ and one NP value of $\varepsilon_R^{N\nu}$. As the reference level the νSM $s2$ solution (see Fig. 1) is taken for which $\Phi_{\nu SM} = \pi$ (up to the influence of $\delta = 0.80\pi$ equal to $-4.09 \times 10^{-4}\ \pi$).

Interestingly, for the old νSM global analysis [26] with the central value $\sin^2\theta_{13} = 0.010$ (but when the non-zero value of θ_{13} was still disputed), the GP analysis had suggested that the condition $\Phi = \pi$ requires $\sin^2\theta_{13}$

to be enlarged approximately to 0.0175, which value was then inside $\pm 1\sigma$ limits, or alternatively that $\sin^2\theta_{23}$ shall be diminished from 0.51 to 0.506 [26].

B. Geometric phase in NP: The bounds on the CC and NC right-chiral coupling constants ε_R and $\varepsilon_R^{N\nu}$ are given in the Introduction. In Fig. 2, the difference $\Delta\Phi = \Phi_{NP} - \Phi_{\nu\mathrm{SM}}$ between NP and νSM values of Φ as the function of ε_R is depicted. Each curve corresponds to the different value of the phase δ. The upper impact of ε_R on Φ/π is of 10^{-6} order. Even weaker is the influence of $\varepsilon_R^{N\nu}$. Yet, because it enters linearly into the Hamiltonian (6) [18], it therefore depends on the $\varepsilon_R^{N\nu}$ sign, too.

Finally, let us comment on the Majorana neutrino case. In the case of νSM, there is no difference between GP for the Dirac and Majorna neutrinos [5]. In the case of NP, the difference $\Delta^{M-D}\Phi = \Phi^M - \Phi^D$ of the geometric phases Φ^M and Φ^D for the Majorana neutrino and Dirac neutrino is depicted in Fig. 3 as a function of the NP couplings [18]. The impact of $\varepsilon_R^{N\nu}$ and ε_R on Φ/π is of order 10^{-4} and 10^{-5}–10^{-6}, respectively.

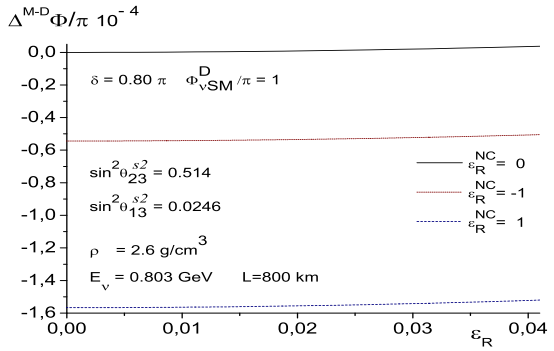


FIG. 3: Comparison of geometric phases for the Majorana and Dirac NP neutrinos. The geometric phase difference $\Delta^{M-D}\Phi = \Phi^M - \Phi^D$ is depicted as a function of the NP coupling constant ε_R. Each curve corresponds to one value of $\varepsilon_R^{N\nu}$.

IV. Conclusions. With this brief paper we have shown that selected properties of the nonadiabatic noncyclic flavor neutrino oscillation can be analyzed in terms of the type of the Aharonov-Anandan GP introduced in [6]. At first, using the trace distance D, it has been checked that in one oscillation period, the muon neutrino state performs the evolution along the path in its Hilbert space, which shows some small departure from cyclicity. Hence the solid angle encircled in this space is close to $2\,\pi$ (similar to the spin particle moving in the mesoscopic ring [27]). This motivates the use of the kinematic approach to the geometric phase presented in [6] which attaches the geometric phase to the Pancharatnam relative one. As mentioned above, the described pattern of the interference in the energy space of the massive neutrino states is highly possible [1, 5]. This in [1] enables us to use the Pancharatnam relative phase for the explanation of the orthogonality of the two-flavor mixing matrix. In [5], the behavior of the GP attached to it was analyzed. In this paper it is pointed out that the present-day global analysis of the oscillation parameters [8] is consistent with the GP value equal to π, which is the reflection of both the unitarity of the mixing matrix and the values of its experimentally estimated parameters. The GP is sensitive to changes of $\sin^2\theta_{23}$ and $\sin^2\theta_{13}$ (see Fig. 1), currently the more disputed parameters [8], whereas the influence of the other νSM oscillation parameters is approximately of the relative order 10^{-6}–10^{-4} in their 2σ ranges. The NP corrections connected with the right-chiral CC and NC currents are at most of the relative order of 10^{-6}, being at present far beyond the experimental verification. Recent progress in entirely novel experimental techniques makes the verification of presented findings more realistic in the future. In the long term, our research may provide new tools for analysis of neutrino physics.

Acknowledgments: The work supported by the NCN Grants No. N202 052940 and No. DEC-2011/01/B/ST6/07197.

[1] P. Mehta, Phys. Rev. D **79**, 096013 (2009); P. Mehta, arXiv:0907.0562v2.
[2] C. Giunti, C.W. Kim, *Fundamentals of Neutrino Physics and Astrophysics* (Oxford University Press, New York, 2007).
[3] M. Ochman, R. Szafron, and M. Zrałek, J. Phys. G **35**, 065003 (2008).
[4] J. Syska, S. Zając, and M. Zrałek, Acta Phys. Pol. B **38**, 3365 (2007).
[5] J. Dajka, J. Syska, and J. Łuczka, Phys. Rev. D **83**, 097302 (2011).
[6] D. M. Tong, E. Sjöqvist, L. Kwek, and C. Oh, Phys. Rev. Lett. **93**, 080405 (2004).
[7] Y. Aharonov and J. Anandan, Phys. Rev. Lett. **58**, 1593 (1987).
[8] D.V. Forero, M. Tórtola, and J.W. F. Valle, Phys. Rev. D **86**, 073012 (2012).
[9] S. Pascoli and T. Schwetz, Adv. High Energy Phys. **2013**, 503401 (2013).
[10] M.C. Gonzalez-Garcia, M. Maltoni, J. Salvado, and T. Schwetz, J. High Energy Phys. 12 (2012) 123; S.K. Raut, arXiv:1209.5658.
[11] Y. Itow, Nucl. Phys. B, Proc. Suppl. **235-236**, 79 (2013).
[12] R. Abela, Nucl. Phys. **A395**, 413 (1983); W. Fetscher, Phys. Lett. **140B**, 117 (1984). K. Nakamura et al. (Particle Data Group), J. Phys. G **37**, 075021 (2010).
[13] J.F. Bueno et al., Phys. Rev. D **84**, 032005 (2011).
[14] S. M. Berman, Phys. Rev. Lett. **1**, 468 (1958); T. Kinoshita, Phys. Rev. Lett. **2**, 477 (1959); W.J. Marciano and A. Sirlin, Phys. Rev. Lett. **71**, 3629 (1993).
[15] B. A. Campbell and D.W. Maybury, Nucl. Phys. **B709**, 419 (2005).

[16] G. Ecker, J. Gasser, A. Pich, and E. De Rafael, Nucl. Phys. **B321**, 311 (1989); J.F. Donoghue, E. Golowich, B.R. Holstein, *Dynamics of the Standard Model*, (Cambridge University Press, Cambridge, England, 2002); B.A. Campbell, A. Ismail, hep-ph/0810.4918 (2008).

[17] Z. Maki, M. Nakagawa, and S. Sakata, Prog. Theor. Phys. **28**, 870 (1962); B. Pontecorvo, JETP **26**, 984 (1968).

[18] F. del Aguila, J. Syska, and M. Zrałek, Phys.Rev. D **76**, 013007 (2007).

[19] M. C. Gonzalez-Garcia and M. Maltoni, Phys. Rev. D **70**, 033010 (2004).

[20] D. Chrusciński and A. Jamiołkowski, *Geometric Phases in Classical and Quantum Mechanics*, (Birkhäuser, Berlin, 2004).

[21] V.A. Naumov, Phys.Lett B **323**, 351 (1994); X.-G. He, X.-Q. Li, B. McKellar, and Y. Zhang, Phys. Rev. D **72**, 053012 (2005).

[22] M.V. Berry, Proc. R. Soc. A **392**, 45 (1984).

[23] N. Nakagawa, Ann. Phys (N.Y.) **179**, 145 (1987).

[24] S. Pancharatnam, Proc. Indian Acad. Sci. A **44**, 247 (1956).

[25] M.A. Nielsen and L.I. Chuang, *Quantum Computation and Quantum Information* (Cambridge University Press, Cambridge, England, 2000).

[26] T. Schwetz, M. Tórtola, and J.W.F. Valle, New J. Phys. **13**, 063004 (2011); hep-ph/1103.0734v2.

[27] T.-Z. Qian and Z.-B. Su, Phys. Rev. Lett. **72**, 2311 (1994).